10 Temporal dynamics of coastal Antarctic phytoplankton: environmental driving forces and impact of a 1991/92 summer diatom bloom on the nutrient regimes

MARK A. MOLINE[1], BARBARA B. PRÉZELIN[1], OSCAR SCHOFIELD[1] AND RAYMOND C. SMITH[2]

[1]Marine Primary Productivity Group, Department of Biological Sciences and Marine Science Institute, University of California, Santa Barbara, CA 93106, USA, [2]Department of Geography, the CSL/Center for Remote Sensing and Environmental Optics, and the Marine Science Institute, University of California, Santa Barbara, CA 93106, USA

ABSTRACT

Within the Palmer Long Term Ecological Research Program (PAL-LTER), a suite of environmental data sets were collected at a nearshore station throughout the 1991/92 austral summer. Seasonal changes are presented in the context of phytoplankton community ecology. Subseasonal fluctations in sea-ice coverage, freshwater inputs, as well as wind driven and advective processes disrupting stratified surface waters, appeared to be the major driving forces affecting the timing, duration and demise of local phytoplankton blooms. During a large diatom-dominated bloom (~30 mg chl a m^{-3}), macronutrients were depleted to detection limits ($NO_3^- < 0.05$ mmol m^{-3}, $PO_4^{3-} < 0.03$ mmol m^{-3}) and significant shifts in nutrient ratios were observed. Phytoplankton populations were light limited below ~5 m during the bloom, resulting from self-shading. The depth of light limitation deepened after the bloom was physically disrupted and removed from the region by strong advective processes.

Key words: phytoplankton, Antarctica, bloom, time series, nutrient limitation, mixed layer depths, photoadaptation, light limitation

INTRODUCTION

Recent studies have integrated physical, chemical and biological data in an attempt to understand the mechanisms controlling phytoplankton bloom dynamics in the Southern Ocean (Smith & Sakshaug 1990, Holm-Hansen & Mitchell 1991, Mitchell & Holm-Hansen 1991, Sakshaug *et al.* 1991). Theories and empirical models derived from such studies suggest that resource limitation and/or water column stability are the major factors governing phytoplankton bloom dynamics. Most studies have been conducted shipboard in pelagic regions and have focused on describing the short-term spatial variability of phytoplankton distribution, abundance, productivity and physiology. Temporal variations in bloom dynamics on the timescale of weeks are less documented (however, see Whitaker 1982, Krebs 1983, Priddle *et al.* 1986, Mitchell & Holm-Hansen 1991) and are generally based on a limited number of environmental parameters and/or insufficient information to track variations on the timescale of a few days over an entire season.

With the PAL-LTER data set from the summer 1991/92 season, we have just that opportunity. Here, we document the occurrence of a large bloom and present a detailed study of phytoplankton dynamics off the coast of Anvers Island on subseasonal timescales ranging from days to months within the summer season. By examining these variations on timescales of days, we hope to advance the understanding of the mechanisms regulating phytoplankton productivity and bloom development in Antarctic coastal waters.

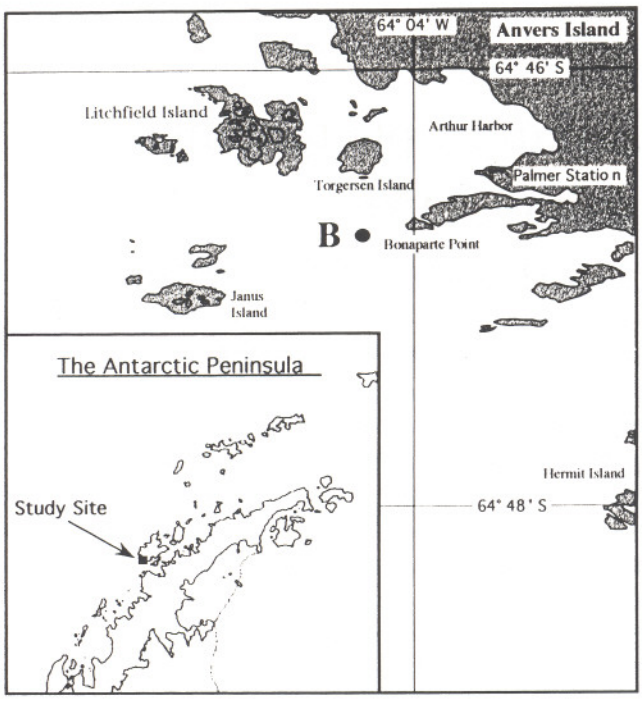

Fig. 10.1. Location of LTER sampling station B (64° 46.45' S, 64° 03.27' W) with respect to Palmer Station and (inset) the Antarctic Peninsula.

MATERIALS AND METHODS

Between November 1991 and February 1992, a total of 257 discrete water samples were collected repeatedly from Station B (Sta B) in the nearshore waters adjacent to Palmer Station, Antarctica (Fig. 10.1). Daily precipitation, snow cover and average wind speed and direction measurements were made at Palmer Station during the study period. These measurements were part of a longterm database collected by the US National Science Foundation. Prior to sample collection, in-water irradiances of photosynthetically available irradiation (Q_{par}) were made with a Biospherical Scalar Irradiance Meter (QSR-170DT) equipped with a QSP-100DT underwater sensor, deployed from an inflatable Zodiac boat. Samples were collected in 5l GoFlo bottle, transferred to dark carboys and immediately returned to Palmer Station for analyses.

Replicate subsamples for nutrient determination were filtered within an hour of collection through a 0.2 μm Nuclepore membrane, and the 20 ml filtrate for each sample was stored in polycarbonate scintillation vials (acid washed) at −70 °C. Samples were later transported at −20 °C to the Marine Science Analytical Laboratories, University of California, Santa Barbara for nutrient analyses. Methods for determination of the dissolved inorganic NO_3^-, PO_4^{3-}, and $Si(OH)_4$ concentrations were those of Johnson *et al.* (1985).

Reverse-phase HPLC procedures of Bidigare *et al.* (1989) were followed to determine the abundance of 17 phytoplankton pigments. Replicate 1 litre samples were filtered on 0.4 μm nylon 47 mm Nuclepore filters and extracted in 3 ml 90% acetone for 24 h in the dark (–20 °C). Pigment separation was carried out with a Hitachi L-6200A liquid chromatograph (436 nm). Peak identities of algal extracts were determined by comparing their retention times with pure pigment standards.

Blue-green photosynthetron methods described by Prézelin *et al.* (1994) were used to determine photosynthesis–irradiance (P–I) relationships for 77 of the collected samples. Non- linear curve fits for P–I data were calculated using the simplex method of Caceci & Cacheris (1984). Curve fitting provided estimates of P_{max} (the light saturated rate of photosynthesis), α (the affinity for photosynthesis at light-limited irradiances) and $I_k = P_{max}/\alpha$ (an estimate of the minimum irradiance required to light saturate photosynthesis).

Physical data were collected with instrumentation on a second inflatable Zodiac boat described by Smith *et al.* (1992). A total of 21 conductivity and temperature profiles were collected at Sta B using a SeaBird CTD. Here, we make a preliminary estimate of the upper mixed layer (UML) based on Sigma-t (σ_t) plots derived from these profiles, using the formula

$$\max\left|\frac{d\sigma_t}{dz}\right|$$

which assumes the UML depth to be equal to the depth where the gradient in σ_t is maximal. Like Mitchell & Holm-Hansen (1991), we assume that if the maximal σ_t gradient was less than 0.05 per metre, then the water column is essentially well mixed to the bottom (*c.* 80 m at Sta B).

There were several occasions when a freshwater lens was clearly evident on top of the marine layer. In these instances, an estimate of the mixing depth of the freshwater lens (FW-MLD) was made in addition to the UML depth.

Contour Plots were generated using the Delaunay triangulation method (DeltaGraph Pro3, DeltaPoint Inc., Monterey, CA, USA).

RESULTS

Until mid-December, the water column at Sta B was routinely covered with ice, buffered from relatively weak local winds, isothermal (–1.3 °C) and mixed to the bottom (Fig. 10.2). Glacier calving and a major wind event combined to break up and blow out local fast ice in mid-December. Due to solar insolation, ice-free conditions, major snow and glacier melt and precipitation, a freshwater lens (σ_t=26–26.6) developed and persisted throughout the summer season (Fig. 10.2). In addition to the effects of freshwater, relatively low wind speeds (<5 m s^{-1}) recorded through the first week in January allowed the water column to stratify and the UML shallowed to 20 m. Surface water temperature within the FW-MLD had warmed to +1.3 °C during this time, while within the UML, below the FW-MLD, the temperature was *c.* −0.2 °C (data not shown). Storm activity, beginning the second week of January, produced high precipitation and maintained strong northerly winds (av. ~15 m s^{-1}) for the following two weeks (Fig. 10.2). Water stratification broke down and within four days, the UML depth deepened to 55 m. Temperature–salinity relationships over the season indicate that

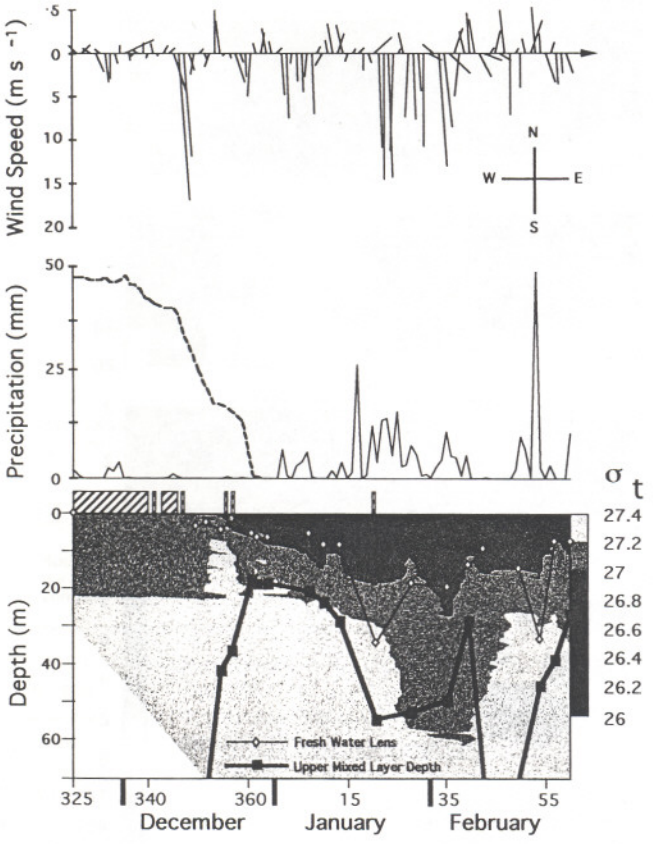

Fig. 10.2. (upper) Seasonal changes in daily average wind speed and direction at Palmer Station between November 21, 1991 and February 27, 1992. Inserted compass provides direction toward which the wind is blowing. (middle) Seasonal patterns in daily precipitation (solid line) and relative snow cover (dashed line) at Palmer Station. (lower) Seasonal contour plot of sigma-t (σ_t) at Station B, indicated by shading; see scale on the right. Seasonal changes in the depth of the upper mixed layer (black squares) and the freshwater lens (open diamonds) overlay the σ_t contour. Daily presence or absence of pack ice is indicated by the hatched bars.

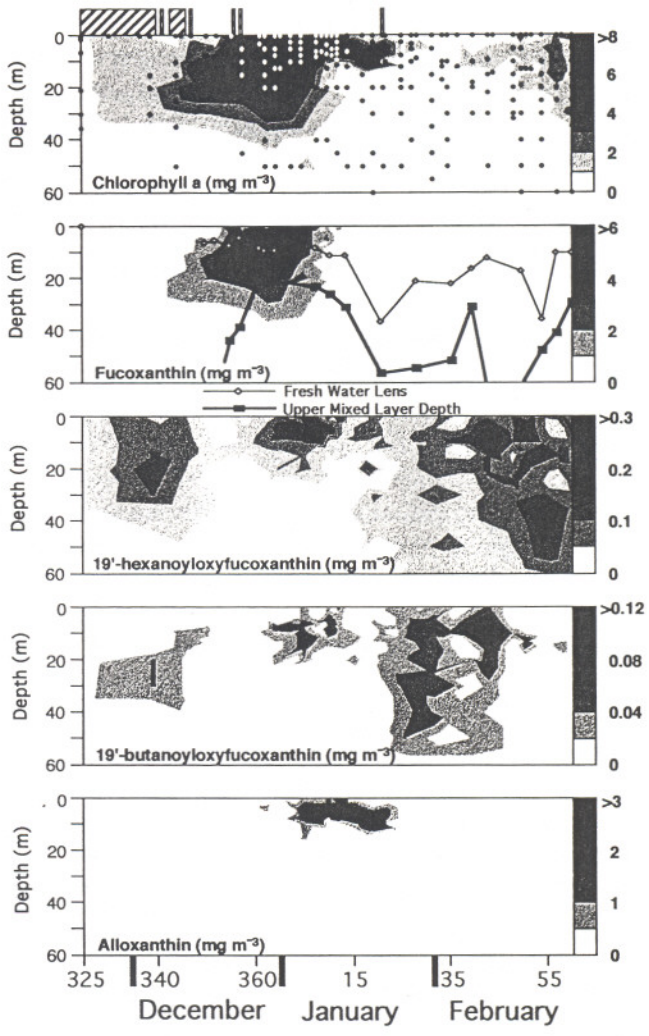

Fig. 10.3. Comparison of the seasonal changes in the depth distribution of chlorophyll *a* and of key phytoplankton pigments at Station B between November 21, 1991 and February 27, 1992. Pigments shown are indicators for diatoms (fucoxanthin), prymnesiophytes (19'-hexanoyloxyfucoxanthin), chrysophytes (19' butanoyloxyfucoxanthin), and cryptophytes (alloxanthin). Pigment concentrations are shown by shading; see scale on the right. Distribution of discrete samples is shown with closed circles in the upper panel. Seasonal changes in the depth of the upper mixed layer (black squares) and the freshwater lens (open diamonds) are shown in the second panel. The daily presence or absence of pack ice is indicated by the hatched bars.

a different water mass was advected into the area during this period (data not shown). With variable winds, the UML depth fluctuated and was not stable until mid February.

Concentrations of chlorophyll *a* (mg chl *a* m^{-3}) at Sta B varied 340-fold over the summer period, ranging from 0.086 to 29.2 mg m^{-3} (Fig. 10.3). Integrated water column values ranged from 59 to 612 mg chl *a* m^{-2}, with up to 70% of the biomass below the UML (Fig. 10.4). Early summer communities, present under the ice, were dominated by prymnesiophytes (indicated by 19′-hexanoyloxyfucoxanthin) and chrysophytes (19′-butanoyloxyfucoxanthin) (Fig. 10.3). In mid to late December, coincident with the shallowing of the UML depth to *c.* 20 m, a large diatom-dominated (fucoxanthin) bloom developed at Sta B (Fig. 10.3). For three weeks, the bloom intensified with the highest chl *a* concentrations being observed between 0–10 m. Taxonomic identification indicated bloom samples were dominated by a centric diatom, *Coscinodiscus* spp. (D. Karentz, pers. commun.). Within the last week of the bloom, there was a ten-fold increase in the abundance of prymnesiophyte pigmentation and a corresponding decrease in diatom abundance. The presence of single-celled *Phaeocystis* spp. was confirmed (D. Karentz, pers. commun.). During the second week of 1992 and corresponding to the advection event described above, chl a and all other pigments showed a rapid decrease, with the exception of significant surface concentrations of cryptophytes (alloxanthin) present for a week after the bloom disappearance. Chrysophyte communities were found until the beginning of February when *Phaeocystis* became dominant. As the UML depth began to shallow at the end of the summer monitoring period, diatoms were once again evident.

NO_3^-, PO_4^{3-} and $Si(OH)_4$ concentrations and the corresponding molar ratios of $Si(OH)_4$:NO_3^- and NO_3^-:PO_4^{3-} showed dramatic changes over the season (Fig. 10.5). Associated

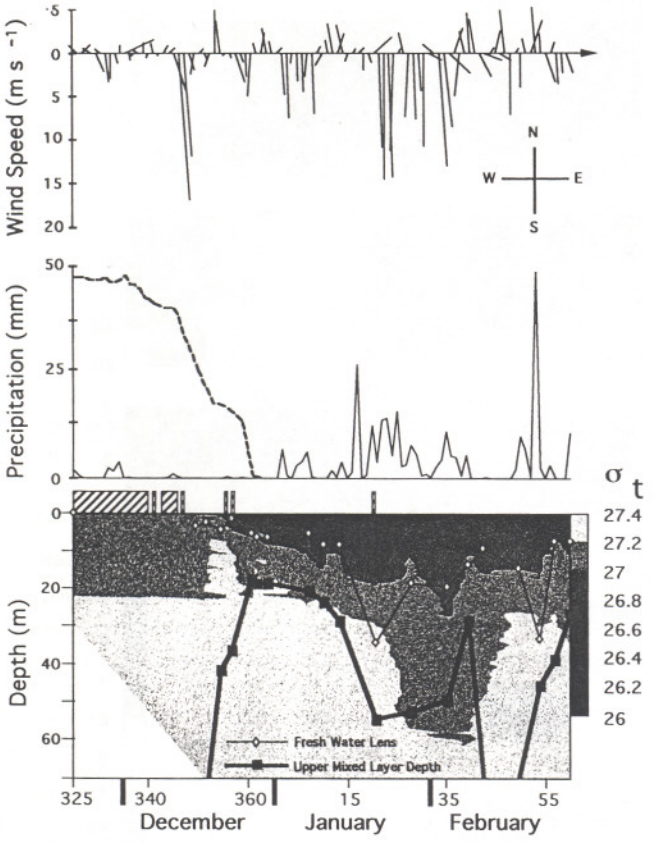

Fig. 10.2. (upper) Seasonal changes in daily average wind speed and direction at Palmer Station between November 21, 1991 and February 27, 1992. Inserted compass provides direction toward which the wind is blowing. (middle) Seasonal patterns in daily precipitation (solid line) and relative snow cover (dashed line) at Palmer Station. (lower) Seasonal contour plot of sigma-t (σ_t) at Station B, indicated by shading; see scale on the right. Seasonal changes in the depth of the upper mixed layer (black squares) and the freshwater lens (open diamonds) overlay the σ_t contour. Daily presence or absence of pack ice is indicated by the hatched bars.

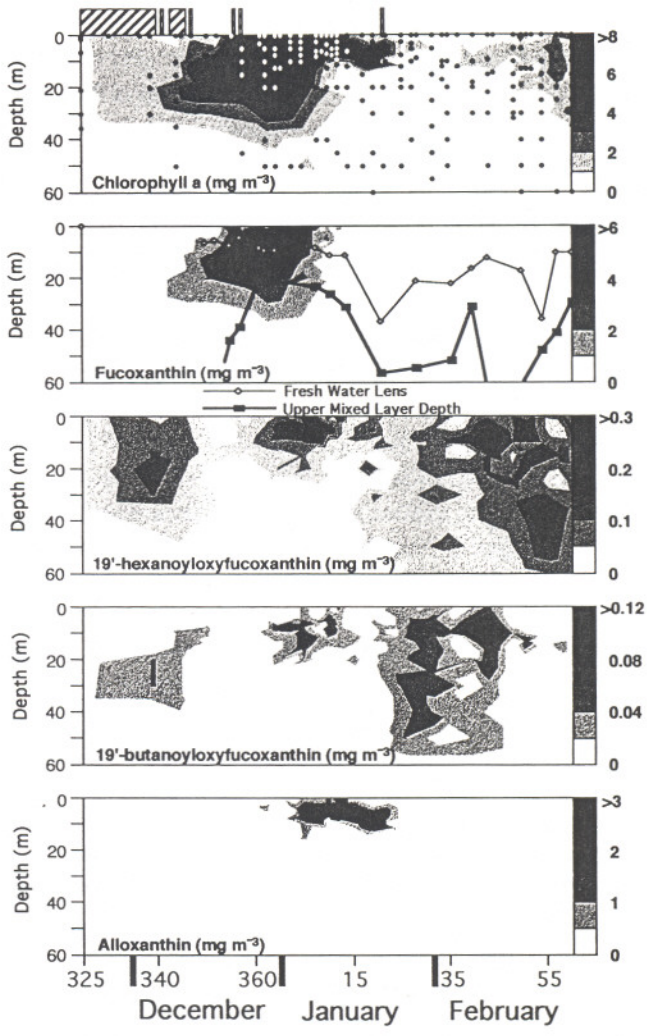

Fig. 10.3. Comparison of the seasonal changes in the depth distribution of chlorophyll *a* and of key phytoplankton pigments at Station B between November 21, 1991 and February 27, 1992. Pigments shown are indicators for diatoms (fucoxanthin), prymnesiophytes (19'-hexanoyloxyfucoxanthin), chrysophytes (19' butanoyloxyfucoxanthin), and cryptophytes (alloxanthin). Pigment concentrations are shown by shading; see scale on the right. Distribution of discrete samples is shown with closed circles in the upper panel. Seasonal changes in the depth of the upper mixed layer (black squares) and the freshwater lens (open diamonds) are shown in the second panel. The daily presence or absence of pack ice is indicated by the hatched bars.

a different water mass was advected into the area during this period (data not shown). With variable winds, the UML depth fluctuated and was not stable until mid February.

Concentrations of chlorophyll *a* (mg chl *a* m^{-3}) at Sta B varied 340-fold over the summer period, ranging from 0.086 to 29.2 mg m^{-3} (Fig. 10.3). Integrated water column values ranged from 59 to 612 mg chl *a* m^{-2}, with up to 70% of the biomass below the UML (Fig. 10.4). Early summer communities, present under the ice, were dominated by prymnesiophytes (indicated by 19'-hexanoyloxyfucoxanthin) and chrysophytes (19'-butanoyloxyfucoxanthin) (Fig. 10.3). In mid to late December, coincident with the shallowing of the UML depth to *c.* 20 m, a large diatom-dominated (fucoxanthin) bloom developed at Sta B (Fig. 10.3). For three weeks, the bloom intensified with the highest chl *a* concentrations being observed between 0–10 m. Taxonomic identification indicated bloom samples were dominated by a centric diatom, *Coscinodiscus* spp. (D. Karentz, pers. commun.). Within the last week of the bloom, there was a ten-fold increase in the abundance of prymnesiophyte pigmentation and a corresponding decrease in diatom abundance. The presence of single-celled *Phaeocystis* spp. was confirmed (D. Karentz, pers. commun.). During the second week of 1992 and corresponding to the advection event described above, chl a and all other pigments showed a rapid decrease, with the exception of significant surface concentrations of cryptophytes (alloxanthin) present for a week after the bloom disappearance. Chrysophyte communities were found until the beginning of February when *Phaeocystis* became dominant. As the UML depth began to shallow at the end of the summer monitoring period, diatoms were once again evident.

NO_3^-, PO_4^{3-} and $Si(OH)_4$ concentrations and the corresponding molar ratios of $Si(OH)_4$:NO_3^- and NO_3^-:PO_4^{3-} showed dramatic changes over the season (Fig. 10.5). Associated

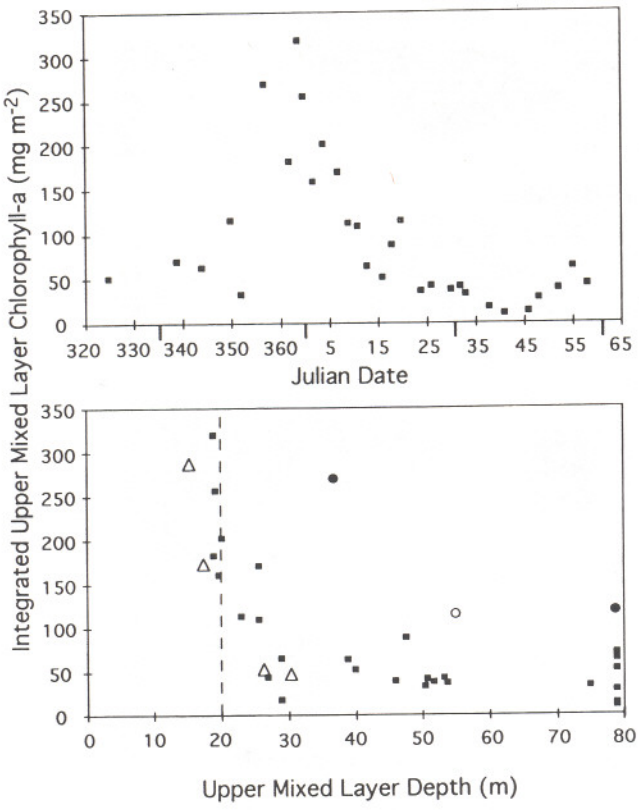

Fig. 10.4. Variations in integrated chl *a* above the upper mixed layer depth (UML) displayed as a function of time over the austral summer (upper) and UML (lower) for Station B, sampled between November 21, 1991 and February 27, 1992. In the lower panel, discrete data points within the PAL-LTER dataset have been differentially labelled (by closed squares) to indicate integrated chl *a* values present prior to the major shallowing of the UML (closed circles) noted in December, 1991 (Fig. 10. 2) and one value during a major advection event in late January, 1992 (open circle). For comparison, monthly mean values (open triangles), derived from chl *a* and σ_t profiles collected along the Antarctic Peninsula between December 1986 and March 1987, are presented (Mitchell & Holm-Hansen 1991). Dashed line represents UML depth in late Dec./early Jan.

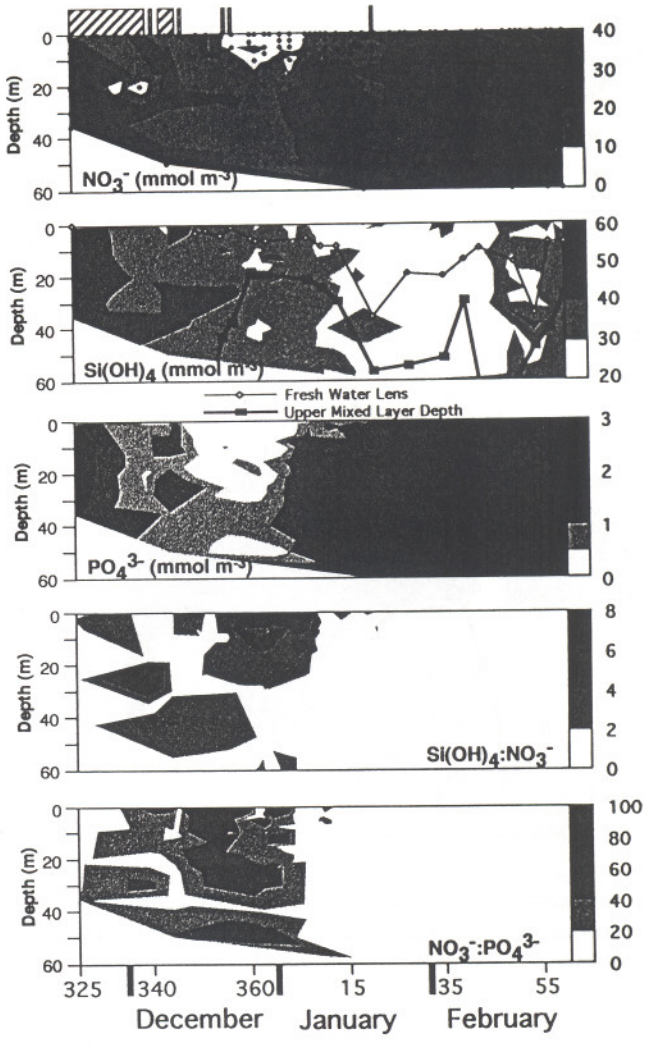

Fig. 10.5. Comparison of the seasonal changes in the depth distribution of the major macronutrients NO_3^-, $Si(OH)_4$ and PO_4^{3-}, and the derived molar ratios for $Si(OH)_4$:NO_3^- and NO_3^-:PO_4^{3-} determined for discrete samples (closed circles) collected at Station B between November 21, 1991 and February 27, 1992. Seasonal changes in the depth of the upper mixed layer (black squares) and the freshwater lens (open diamonds) are shown in the second contour plot. The daily presence or absence of pack ice is indicated by the hatched bars.

with the bloom was a depletion of NO_3^- and PO_4^{3-} to detection levels (PO_4^{3-}<0.03 mmol m^{-3}, NO_3^-<0.05 mmol m^{-3}). The ratio of NO^{-3}:PO_4^{3-} also increased during the bloom and the difference in this ratio between 'nonbloom' (x=14.14±2.99, n=166) and bloom waters (x=48.65±28.66, n=51) was found to be significant at p<0.01 (Fig. 10.6). The large increase in the NO_3^-:PO_4^{3-} ratio was due to the disproportionately large uptake of PO_4^{3-} by phytoplankton. After the bloom and coincident with the advection event, PO_4^{3-} and NO_3^- concentrations returned to pre-bloom levels.

The early summer period was characterized by high levels of $Si(OH)_4$ throughout the water column below the ice (Fig. 10.5) when diatoms were not abundant (Fig. 10.3). During the diatom bloom, $Si(OH)_4$ concentrations throughout the water column were reduced from >40 mmol m^{-3} to <30 mmol m^{-3}. High $Si(OH)_4$:NO_3^- ratios during the bloom were primarily due to the large reduction of NO_3^- in the highly stratified UML. Following the bloom and advection of different water masses into the region, $Si(OH)_4$ concentrations thoughout the water column showed a further reduction (Fig. 10.5). Only in late February did $Si(OH)_4$ concentrations begin to rise.

Fig. 10.7 shows the phytoplankton's photoadaptive state over the season. Phytoplankton were light limited (Q_{par}/I_k >1) below 20 m for the entire season; however, the depth of light limitation shallowed to ~5 m during the bloom.

DISCUSSION

Results from this study document phytoplankton dynamics on timescales of days and illustrate the linkages and feedback mechanisms between the biological, physical and chemical environments. Seasonal freshwater inputs and decreased local winds caused stratification of the water column, which has been found in other studies to be a major controlling factor initiating biomass growth (Whitaker 1982, Smith & Sakshaug 1990,

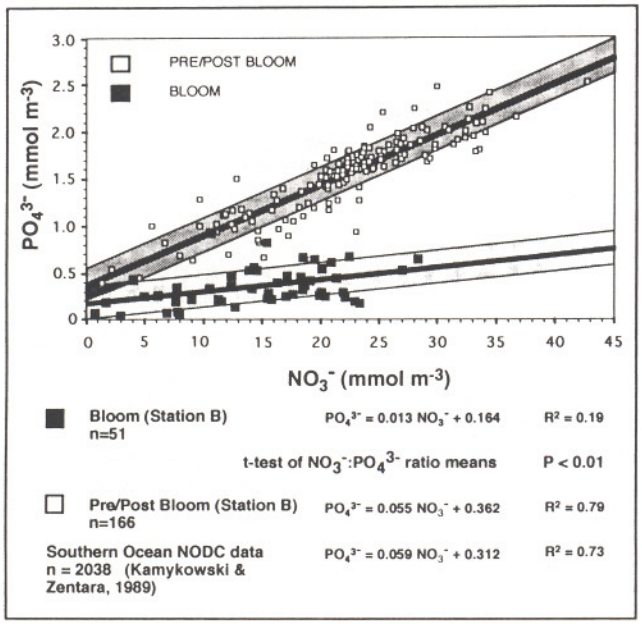

Fig. 10.6. Comparison of regression plots for changes in the abundance of inorganic NO_3^- and PO_4^{3-} for all depths sampled at Station B between November 21, 1991 and February 27, 1992. One regression line represents the PO_4^{3-} to NO_3^- relationship (open squares) for both the pre- and post-bloom period. The other regression represents the PO_4^{3-} to NO_3^- relationship (closed squares) during the diatom-dominated bloom occurring between December 10, 1991 to January 9, 1992 (Fig. 10.3). The shaded areas bordering each regression line represent ± one standard deviation.

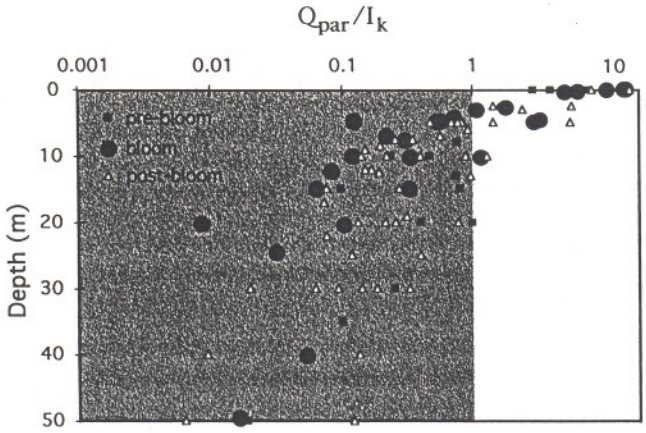

Fig. 10.7. Depth distribution of the photophysiological parameter Q_{par}/I_k determined for discrete samples collected from Station B between November 27, 1991 and February 27, 1992. Productivity measurements made prior (closed squares), during (closed circles) and after (open diamonds) the major diatom bloom are indicated. The shaded area indicates data where light limitation was evident.

Holm-Hansen & Mitchell 1991, Mitchell & Holm-Hansen 1991, Sakshaug *et al.* 1991). Water column stability in December allowed the phytoplankton to photoacclimate and overcome light limitation of growth. Biomass then accumulated in the upper 20 m and resulted in a major diatom bloom. As predicted by Kiefer & Kremer (1981), the zone of maximal growth and biomass shallowed as the bloom progressed. With the increase in biomass and light attenuation, the depth at which the phytoplankton were light limited also shallowed to ~5 m during the bloom (Fig. 10.7). With the shallowing of the UML, there was a shift in the phytoplankton composition from *Phaeocystis* (~1–3 m) to a larger diatom species (*Coscinodiscus* spp. ~40–80 m). Previous studies in the Antarctic have found an identical pattern of transition to larger phytoplankton as water column stability increases (Whitaker 1982, Rivkin 1991).

With the diatom biomass approaching concentrations thought maximal for Antarctic waters (Holm-Hansen *et al.* 1989), the chemical environment was significantly altered. The relationship between PO_4^{3-} and NO_3^- concentrations before and after the bloom was nearly identical to the Southern Ocean NODC (National Oceanographic Data Center) data given by Kamykowski & Zentara (1989) (Fig. 10.6). However, during the bloom, a significant shift in the relationship of NO_3^- to PO_4^{3-} showed the preferential uptake of PO_4^{3-}. Without a vertical nutrient flux caused by the strong stratification, this trend continued to detection limits, and therefore, PO_4^{3-} could have become the limiting resource. When PO_4^{3-} concentrations dropped to detection limits in the upper 10 m there was a change in the phytoplankton community from diatoms to *Phaeocystis*. Antarctic diatoms have shown competitive interactions for limiting nutrients, suggesting that algal assemblages may vary with limited resources (Sommer 1988, 1991), but this is the first study to present evidence that a shift in the nutrient field may result in changes in a natural Antarctic phytoplankton population. The change in the phytoplankton assemblage may have taken place as a result of PO_4^{3-} limiting the growth of *Coscinodiscus* spp., despite relatively high $Si(OH)_4$ concentrations, and the ability of *Phaeocystis* to utilize low concentrations of both PO_4^{3-} and NO_3^-. The nutrient absorption and storage capacity of the mucilage surrounding *Phaeocystis* colonies has been demonstrated in a range of both PO_4^{3-} (Veldhuis *et al.* 1991) and NO_3^- (Verity *et al.* 1988) concentrations and is a possible mechanism to explain the transition from diatoms to *Phaeocystis* in the low macronutrient environment at Sta B.

The dramatic macronutrient shifts in the water column during the second week of January were due to the advection of a different water mass into the area. The PO_4^{3-}-rich, NO_3^--rich and $Si(OH)_4$-poor water mass observed in the latter half of this study could have been a result of water with high PO_4^{3-}, NO_3^- and $Si(OH)_4$ concentrations mixing with coastal glacial meltwater and island runoff with high PO_4^{3-} and NO_3^- concentrations and no $Si(OH)_4$. Such mixing processes would have a diluting affect for $Si(OH)_4$ while not effecting the PO_4^{3-} and NO_3^- concentrations. Supporting evidence for the presence of glacial flour at Sta B is revealed in the σ_t data (Fig. 10.2), indicating a large freshwater input and high light attenuation in the top 20 m in the absence of high biomass (data not shown).

The presence of flagellates (cryptophytes (alloxanthin) and chrysophytes (19'-butanoyloxy-fucoxanthin)) during the month following the advection event may indicate a better adaptability to this period of increased vertical mixing, which has been documented in pelagic regions off the Antarctic Peninsula

(Kopczynska 1992). The final two weeks of the study are of particular interest because it was during this period that a second diatom bloom began to develop. Conditions were very similar to those found earlier in November and December; decreased winds, a shallowing UML and a transition from *Phaeocystis* to diatoms (fucoxanthin increased from <0.1 to 0.5 mg m^{-3}). These conditions initiated a second bloom that continued through the third week in March (Haberman, pers. commun.). Krebs (1983) showed that during a sampling period from December 1971 to January 1974 there were major blooms occurring in December–January and secondary less-intense blooms during the March–April time period. These findings, along with data from this study and from Holm-Hansen *et al.* (1989), suggest that near Palmer Station phytoplankton dynamics and the processes controlling them are similar between years. Physical factors, thought to partially initiate ice-edge blooms, such as a meltwater lens, also appear to be important in coastal systems, providing the stability needed for biomass accumulation. The depth of the UML, as defined in this study, was found to be an important factor in the development of phytoplankton biomass (Fig. 10.4). As the UML shallowed (~20 m), integrated chlorophyll *a* within the UML increased an order of magnitude. Mitchell & Holm-Hansen (1991) also showed the same relationship of increasing biomass with shallowing of the UML (Fig. 10.4). The degree of water column stability appears to also select for certain species: specifically, diatoms in a stratified high-nutrient condition, and *Phaeocystis* and flagellates in a mixed variable nutrient environment prior to stabilization. Although continued analyses of seasonal and interannual data is needed, results from this study give preliminary indications that temporal variations in phytoplankton biomass and community structure result from changes in water column stability and in the nutrient regime, and occur on the equivalent timescales as the transitional events (i.e. mixing, advection, stratification) seen in the physical dynamics.

ACKNOWLEDGEMENTS

K. Seydell, K. Scheppe, P. Handley and T. Newberger are thanked for their assistance in sample collection and analyses. Thanks to J. Priddle and O. Holm-Hansen for helpful comments. We also acknowledge R. Bidigare and M. Ondrusek for providing the HPLC training and pigment standards. Research was supported by National Science Foundation grant DPP 90–901127 to B. B. Prézelin. This is Palmer LTER publication number 47.

REFERENCES

Bidigare, R. R., Schofield, O. & Prézelin, B. B. 1989. Influence of zeaxanthin on quantum yield of photosynthesis of *Synechococcus* clone WH7803 (DC2). *Marine Ecology Progress Series*, **56**, 177–188.

Caceci, M. S. & Cacheris, W. P. 1984. Fitting curves to data. *Byte*, **9**, 340–362.

Holm-Hansen, O., Mitchell, B. G., Hewes, C. D. & Karl, D. M. 1989. Phytoplankton blooms in the vicinity of Palmer Station, Antarctica. *Polar Biology*, **10**, 49–57.

Holm-Hansen, O. & Mitchell, B. G. 1991. Spatial and temporal distribution of phytoplankton and primary productivity in the western Bransfield Strait region. *Deep-Sea Research*, **38**, 961–980.

Johnson, K. S., Petty, R. L. & Thomsen, J. 1985. Flow injection analysis for seawater micronutrients. In Zirino, A., ed. *Mapping Strategies in Chemical Oceanography. Advances in Chemistry Series*, **209**, 7–30.

Kamykowski, D. & Zentara, S. 1989. Circumpolar plant nutrient covariation in the Southern Ocean: patterns and processes. *Marine Ecology Progress Series*, **58**, 101–111.

Kiefer, D. A. & Kremer, J. N. 1981. Origins of vertical patterns of phytoplankton and nutrients in the temperate, open ocean: a stratigraphic hypothesis. *Deep-Sea Research*, **28**, 1087–1105.

Kopczynska, E. E. 1992. Dominance of microflagellates over diatoms in the antarctic areas of deep vertical mixing and krill concentrations. *Journal of Plankton Research*, **14**, 1031–1054.

Krebs, W. N. 1983. Ecology of neritic marine diatoms, Arthur Harbor, Antarctica. *Micropaleontology*, **29**, 267–297.

Mitchell, B. G. & Holm-Hansen, O. 1991. Observations and modeling of the Antarctic phytoplankton crop in relation to mixing depth. *Deep-Sea Research*, **38**, 981–1007.

Prézelin, B. B., Boucher, N. P. & Smith, R.C. 1994. Marine primary production under the influence of the Antarctic ozone hole: Icecolors '90. *Antarctic Research Series*, **62**, 159–186.

Priddle, J., Heywood, R. B. & Theriot, E. 1986. Some environmental factors influencing phytoplankton in the Southern Ocean around South Georgia. *Polar Biology*, **5**, 65–79.

Rivkin, R. B. 1991. Seasonal patterns of planktonic production in McMurdo Sound, Antarctica. *American Zoology*, **31**, 5–16.

Sakshaug, E., Slagstad, D. & Holm-Hansen, O. 1991. Factors controlling the development of phytoplankton blooms in the Antarctic Ocean – a mathematical model. *Marine Chemistry*, **35**, 259–271.

Smith, R. C., Baker, K. S., Handley, P. & Newberger, T. 1992. Palmer LTER program: hydrography and optics within the Peninsula grid, Zodiac sampling grid during the 1991–1992 field season. *Antarctic Journal of the United States*, **27**, 253–255.

Smith Jr., W. O. & Sakshaug, E. 1990. Polar Phytoplankton. In Smith, W.O. ed. *Polar oceanography; Part A: Physical science. Part B: Chemistry, biology, geology*. San Diego: Academic Press, 477–526.

Sommer, U. 1988. The species composition of Antarctic phytoplankton interpreted in terms of Tilman's competition theory. *Oecologia*, **77**, 464–467.

Sommer, U. 1991. Comparative nutrient status and competitive interactions of two Antarctic diatoms (*Corethron criophilum* and *Thalassiosira antarctica*). *Journal of Plankton Research*, **13**, 61–75.

Veldhuis, M. J. W., Colijn, F. & Admirall, W. 1991. Phosphate utilization in *Phaeocystis pouchetii* (Haptophyceae). *Marine Ecology*, **12**, 53–62.

Verity, P. G., Villareal, T. A. & Smayda, T. J. 1988. Ecological investigations of blooms of colonial *Phaeocystis pouchetii*. I. Abundance, biochemical composition, and metabolic rates. *Journal of Plankton Research*, **10**, 219–248.

Whitaker, T. M. 1982. Primary production of phytoplankton off Signy Island, South Orkneys, the Antarctic. *Proceedings of the Royal Society London*, **B214**, 169–189.